Proceedings of the 21st International Conference on Low Temperature Physics
Prague, August 8-14, 1996
Part S6 – Plenary and invited papers

Raman Scattering as a Probe of the Superconducting Proximity Effect

L. H. Greene [a*], J. F. Dorsten [b*#], I. V. Roshchin [a*], A. C. Abeyta [a*], T. A. Tanzer [b*#+], G. Kuchler [a*], W. L. Feldmann [a*], and P. W. Bohn [b*#]

[a] *Department of Physics and the Materials Research Laboratory, University of Illinois at Urbana-Champaign, Urbana, IL 61801, USA*

[b] *Department of Chemistry and the Materials Research Laboratory, University of Illinois at Urbana-Champaign, Urbana, IL 61801, USA*

Temperature-dependent Raman spectroscopy is used to investigate the effect of superconductivity on the near-surface electronic structure of a semiconductor in good electrical contact with a superconductor. The light scattering is performed through a high-quality thin (60-100Å) film of Nb, grown directly onto *in-situ* Ar^+-etched (100)-n^+InAs. Below T_c, the LO mode, associated with the surface charge accumulation layer in the InAs, is enhanced by ~40% in comparison with the nearby L_- bulk phonon mode. This change, reversible upon temperature cycling, is observed only when the Nb is in good electrical contact with the InAs. Preliminary results show a similar effect on NbN/InAs. Our results constitute the first optical detection of the superconducting proximity effect.

1. INTRODUCTION

The superconducting proximity effect [1] has been described as the leakage of Cooper pairs from the superconductor to the normal metal. The spatial extent of the effect on the normal metal and superconducting sides is determined by the normal-metal and superconducting coherence lengths, respectively. Although this effect has been studied for many years, there are still debates over the proper description of this phenomenon. [2,3]

More recently, studies of superconductor/ semiconductor interfaces have been undertaken. [4] The replacement of the normal metal by a semiconductor reveals a great variety of intriguing physical phenomena for investigation. First, the electronic properties of semiconductors are quite disparate from those of normal metals. Typically, the Fermi velocity and the effective mass are on the order of 20 times lower, and the carrier concentration is typically 10^4 - 10^6 times lower in a semiconductor than in a metal. Second, a great advantage over all-metal junctions is that the electronic properties of semiconductors may be tuned over several orders of magnitude by adjusting both the doping level and the choice of semiconductor. Third, and most important for proximity-effect studies, is that the strength of the semiconductor band bending at the interface can be engineered. [5] For most semiconductors, a depletion layer or Schottky barrier forms at the semiconductor interface, and the width is determined by the level of doping. In the case of some narrow-gap semiconductors, such as InAs, bands at the interface bend to form an accumulation of charge, and no Schottky barrier is formed. The width of this charge accumulation region, or CAR, is determined by the Thomas-Fermi screening length.

Support acknowledged by:
* *The Department of Energy through the Materials Research Laboratory # DE-FG02-91-ER45439*
# *The Office of Naval Research # N00014-93-1-1168.*
+ *The Fannie and John Hertz Foundation*

Raman spectroscopy is a proven, powerful probe of the electronic structure in the near-surface region of semiconductors. [6-15] Using visible excitation on highly-doped semiconductors, only the first few tens of angstroms near the surface are probed. Raman-active vibrational modes of the depleted or accumulated surfaces are distinct from the bulk modes because of the differences in their electronic character. Therefore, Raman scattering is effective in comparing the surface electronic properties to those of the bulk. Raman scattering from collective excitations also provides information on the carrier concentration and mobility of free charge carriers in the semiconductor and the band-bending associated with the interface. [9-15] Given these advantages, we have inaugurated the use of Raman scattering to study the effect of superconducting and normal-state Nb films on the near-surface electronic properties of n^+-InAs. [16-18]

2. MOTIVATION and BACKGROUND

A crossover from quasiparticle tunneling to Andreev reflection [19] was studied as a function of Schottky barrier thickness in Nb/InGaAs bilayers by Kastalsky, et. al. [20] For junctions of the highest transmittance, an excess conductance was detected at low bias. The usual mechanisms of quasi-particle tunneling and Andreev scattering at low and high junction transmittances, respectively [21-23], could not account for this excess conductance, and was therefore attributed to a new current-carrying channel at the superconductor / semiconductor interface, namely Cooper pair tunneling. This Cooper pair tunneling was related to earlier work in which a weak excess current was observed in the I-V characteristics of superconductor/insulator/superconductor, S/I/S*, tunnel junctions, where S* was a superconductor, but just above its critical temperature. [24-25] A weak excess current was attributed to a pair-field susceptibility, which manifested itself as a non-equilibrium pair-current across the barrier. In comparison to the effect of pair-field susceptibility, Cooper pair tunneling is larger, and the second electrode may be a normal metal, and not necessarily be a superconductor in its normal state.

The excess conductance at low bias in superconductor/semiconductor junctions was later taken as confirmation of the theory of "reflectionless tunneling" at the interface. [27] This mesoscopic effect relies on *single quasiparticle* phase coherence producing a phase-coherent Andreev reflection. In contrast, Cooper-pair tunneling relies on superconducting *pair* phase coherence. Both mechanisms explain the excess conductance observed in the reported data equally well, but for junctions of higher transmittances, the models predict substantially different behavior in electronic transport. [17,27] Therefore, studies of extremely high-transmittance superconductor/semiconductor junctions of Nb/InAs were undertaken.

Using electron transport techniques, proximity effects have previously been observed in Nb/InAs structures. [28-33] The III-V compound semiconductor InAs was used because, instead of a depletion layer or Schottky barrier, it can form a charge accumulation region (CAR) at its surface, shown schematically in Figure 1. [5] The thickness of this CAR, which is determined by the Thomas-Fermi screening length in the space-charge region, can be measured by Raman spectroscopy. [34]

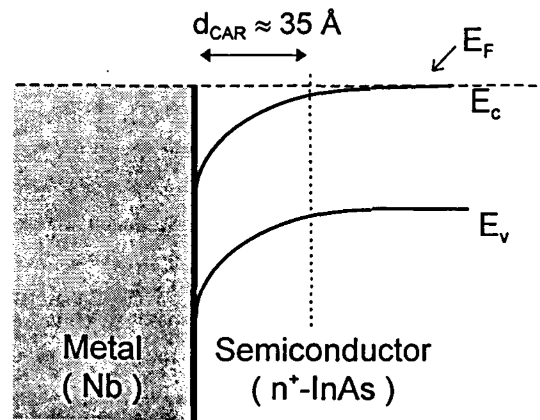

Figure 1: Schematic of the energy band diagram of a Nb/(100)-n^+-InAs bilayer depicting the charge accumulation region (CAR) at the interface. The width of the CAR is measured to be 35 Å for the Sn+S doping of $n=1.2\times10^{19} cm^{-3}$.

Based on studies of the effect of surface reconstruction on the accumulation region, Noguchi et al. [35] proposed that the accumulation region is a result of intrinsic donor-like surface states produced by the surface reconstruction. These changes result in band-bending that is the reverse of that typically observed in n-type III-V materials. The Fermi level is pinned in the conduction band, and electrons are then trapped at the n^+-InAs surface, thereby forming the CAR.

Separate longitudinal Raman modes, associated with the bulk and charge accumulation regions are observed near the (100) InAs surface. Two coupled phonon-plasmon modes, L- and L+, are associated with the bulk InAs. An unscreened LO phonon mode is associated with the charge accumulation region near the surface. This bare LO phonon mode is allowed because the magnitude of the wave vector of the LO phonon in the accumulated region is larger than the Thomas-Fermi wave vector, leaving the LO phonon unscreened. [36-38]

3. EXPERIMENTAL DETAILS

The thin Nb films are grown by planar dc-magnetron sputter deposition in a UHV-compatible stainless-steel vacuum chamber. The base pressure is less than 1×10^{-8} Torr. To remove any oxide layer on the substrate surface before deposition, a gentle *in-situ* Ar^+ etch is performed in an Ar partial pressure of 2×10^{-4} Torr with a 3 cm diameter ion gun at 75 V and 1.0 mA. The Nb films are then grown in an Ar atmosphere of 7×10^{-3} Torr with the sputter gun held at a power of 180 Watts. Single-crystal substrates of highly-doped, n^+-InAs ($n=1.2\times10^{19}cm^{-3}$, Sn+S-doped), nominally undoped InAs ($n=1.8\times10^{16}$ cm^{-3}) and sapphire are used.

The structural quality of the Nb films is remarkably high. X-ray reflectivity measurements reveal that the ~100 Å thick Nb films exhibit a surface roughness of 3-5 Å, or one atomic layer. Under scanning electron microscopy (SEM) at a resolution of 30Å, these films are featureless.

The superconducting transition temperature, T_c, of each Nb film structure is measured using a standard four-probe dc resistance technique. As shown in Fig. 2, the T_c of bulk Nb, 9.2K, is observed for films thicker than 2000Å. A gradual reduction in T_c is observed with decreased film thickness and below ~400Å, a dramatic drop in T_c with decreasing thickness occurs. The T_c for each set of samples is measured both prior to and after the Raman experiments and a decrease in T_c of a few tenths of a degree is seen, which we attribute to some surface oxidation.

Raman spectra are collected in a near-backscattering geometry. An Ar^+ laser operated at one of several wavelengths is focused on the sample with a cylindrical lens, giving irradiances ranging from 50-270 W/cm^2. The variation in the irradiances arises from the change in power available at different excitation wavelengths and the need to minimize laser-induced heating. All signal calculations are normalized to constant irradiance. A triple grating spectrometer equipped with a charge coupled device (CCD) camera is used to analyze the scattered radiation. The analysis is performed in the $x(y,z)\bar{x}$ polarization configuration where x, y, and z represent the (100), (010), and (001) directions, respectively. In this geometry, the LO phonon and the L - and L+ coupled phonon-plasmon modes are allowed. [39]

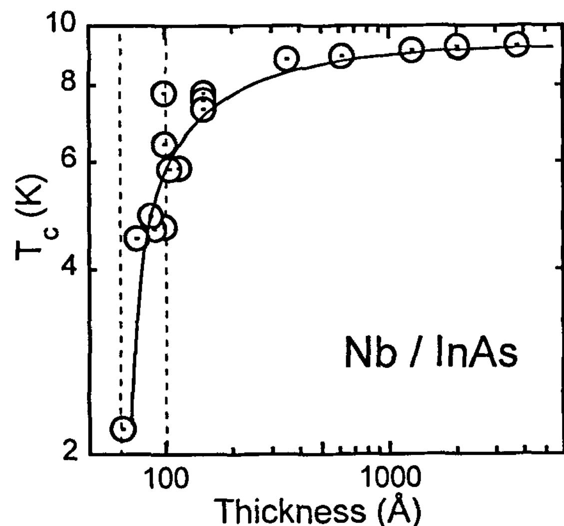

Figure 2: T_c vs. Nb film thickness for Nb/InAs. The solid line is a guide for the eye and the dashed lines indicate the range of film thicknesses used the Raman scattering experiments. [after refs. 16-18]

Measurements are also performed in the $x(y,y)\bar{x}$ configuration where only the LO phonon is allowed. At temperatures near and below T_c, data are taken in an optical cryostat with the Nb/InAs structures immersed in superfluid helium using a Si-diode thermometer buried in the copper block which holds the sample.

4. RESULTS

4.1 Characterization of the InAs surface

The first experiments characterized the InAs before Nb deposition. The thickness of the CAR was determined by Raman spectra taken on bare, room-temperature InAs substrates. Both doped and nominally undoped InAs were measured for comparison. In order to probe a range of sampling depths, excitation wavelengths of 488, 514.5, 496.5 and 457.9 nm were used. The wavelengths, 488, 514.5 nm, are at near-resonance with the E_1 gap of InAs at room temperature, and 496.5 and 457.9 nm are at resonance with the E_1 gap at room temperature and 10K, respectively. Results of the Raman data collected at these different wavelengths are presented in Table 1, where the ratio of scattering from the unscreened LO phonon and the L- collective excitations are shown in relation to the sampling depth.

From the data it is clear that as the sampling depth increases, the ratio of the LO mode to the coupled mode decreases, indicating an increase in scattering from coupled modes. This is clearly seen in the spectra. These results match those reported by Li et al. [37] and support the assertion that the LO mode arises from scattering primarily in the accumulation region while the low-frequency coupled mode is produced from scattering deeper in the bulk. These data, taken with data collected at the same wavelengths on the undoped InAs are used to determine the thickness of the accumulation region. Using an abrupt junction model, the width of the charge accumulation region is determined from $I^{\lambda}(LO) = I_0^{\lambda}\{1 - \exp[-2L_s/d_0(l)]\}$, where I^{λ} and I_0^{λ} are the Raman intensities of the LO phonon from the doped and undoped InAs samples, respectively, L_s is the thickness of the accumulation region, and d_0 is the 1/e penetration depth of the excitation beam. Because these calculations are based on measurements taken from different samples, each Raman intensity measurement consists of an average of at least six measurements taken at different locations to account for surface quality variations and spatial variations in doping. Data from all four excitation wavelengths and different sample locations are used with the abrupt junction model to determine that the width of the charge accumulation region is $d_{car} = 35 \pm 0.3$ Å

Changes in the interface quality of the n^+-InAs due to the Ar^+ etching are detected by taking Raman spectra of a substrate before and after etching. Earlier Raman studies of damage on $In_xGa_{1-x}As$ surfaces by Ar^+ etching showed lineshapes of the InAs-like and GaAs-like LO phonons were weakened and broadened, and at higher damage levels, translational symmetry in the near-surface region was disrupted to the point that the disallowed TO Raman modes were observed. [8]

TABLE I: Intensity ratios of the LO phonon mode to the coupled phonon-plasmon mode based on sampling depth for several wavelengths. Resonance is with the E_1 gap of InAs

	Probe Wavelength (nm)	Sampling Depth (Å)	Intensity ratio I_{LO}/I_{L-}
resonant	457.9	75	1.14
non-resonant	488.0	92	0.71
resonant	496.5	96	0.80
non-resonant	514.5	133	0.58

The Raman spectra of n^+-InAs before and after Ar^+ etching shows that the relative intensity of the LO phonon mode, in comparison to that of the L- mode, is reduced after etching. This result is seen at room temperature using several wavelengths, and at cryogenic temperatures using the 457.9 nm excitation. Raman spectra collected in the $x(y,y)\bar{x}$ geometry, in which the coupled mode is disallowed, show a slight broadening of the LO mode, and the TO mode is not observed. These changes observed in the spectra of our Ar^+-etched InAs substrates are consistent with some induced disorder in the first few atomic layers.

The effects of Nb deposition on the surface of InAs were also studied by measuring the Raman spectra before and after Nb deposition in experiments similar to those reported above. The resulting Raman spectra indicated that Nb deposition causes little change to the etched surface. If the Nb layer is deposited directly on InAs without etching, only a small decrease in the LO mode intensity is observed. In work reported by Corden et. al [40], deposition of thin metal layers on the (110) surface of n^+-InAs and other III-V semiconductors can cause a change in the relative magnitudes of the LO and TO phonon modes, which they attributed to metal-deposition induced disorder in the interfacial region. A comparison to their work indicates that our Nb deposition does not drastically damage the InAs surface.

4.2 Temperature-dependent Raman spectroscopy of Nb/InAs structures.

In order to study the effects of normal-state and superconducting Nb on the interfacial electronic structure of InAs, temperature-dependent Raman spectra of Nb/InAs structures taken through the Nb film are compared. As shown in Fig. 3, upon lowering the sample temperature below T_C, a dramatic increase in the magnitude of LO phonon scattering is observed, while the magnitude of the L- coupled mode decreases. Lineshape-fitting calculations reveal that the observed increase in the magnitude of the LO phonon in comparison to the L_- mode is approximately 40%.

This prominent spectral change is reversible upon cycling through T_C, either by changing the Helium bath temperature or by changing the surface temperature of the Nb/InAs structure with laser fluence. Holding the structure under superfluid helium and increasing the laser fluence causes the ratio of the peak heights to appear as those in the spectrum taken at 10K. Reducing the laser fluence then returns the spectrum to the appearance it has at 2K.

As a control, the same temperature-dependent Raman spectra are taken on the bare InAs surface. Since the Nb is grown as a strip on the InAs substrate, this only requires moving the laser spot to an uncoated region of the substrate. No detectable change in the intensity ratio of the L- coupled mode to the LO mode in the spectrum of the bare InAs surface upon cycling between 10 K and 2 K is observed.

The effects of an insulating barrier between the Nb and InAs are investigated by performing the Raman experiments on a sample in which the native oxide on the InAs surface, believed to be at least 30Å thick, is present.

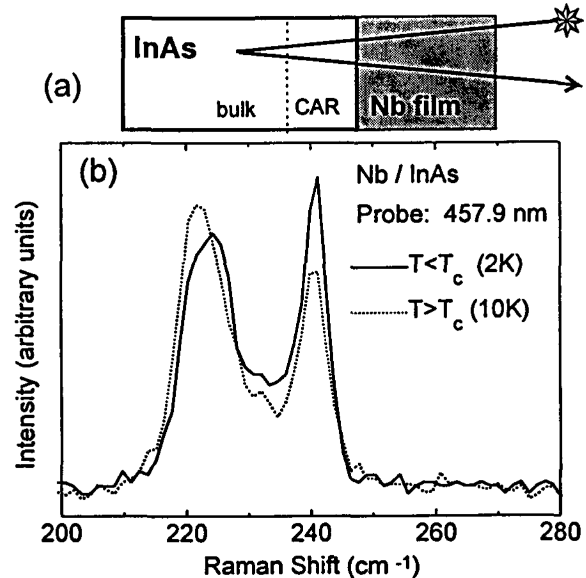

Figure 3. a) Raman spectra are acquired through the Nb film as sketched. b) Raman spectra of a Nb/InAs structure above and below T_C are shown by the dotted and full lines, respectively. Upon cooling from 10K to 2K, the relative intensity of the LO mode is increased by ~40%. [after 16-18]

For this important control experiment, the Nb is grown on the InAs crystal without an Ar^+ etch. In this case, the Raman spectra shows no change in peak intensities upon cycling between 2 K and 10 K. We therefore conclude that the reversible effects observed in the temperature-dependent Raman spectra require good electrical contact between the InAs and Nb.

Another important experiment is to observe this effect with another superconductor. Preliminary data taken on thin NbN_x films grown on InAs show a similar effect as observed with Nb/InAs, as shown in Fig. 4. The NbN_x is chosen for the following reasons. First, the coherence length of NbN is shorter than that of Nb, so the thickness dependence on T_c may not be as drastic as it is in the Nb. Second, NbN_x has a lower carrier-concentration than Nb, so the light can penetrate a thicker NbN_x film. Finally, the superconducting transition temperature of NbN_x is inherently higher than that of Nb. Studies using NbN_x will allow us to do accurate temperature-dependent studies over a wider range than was possible with the Nb/InAs system described here.

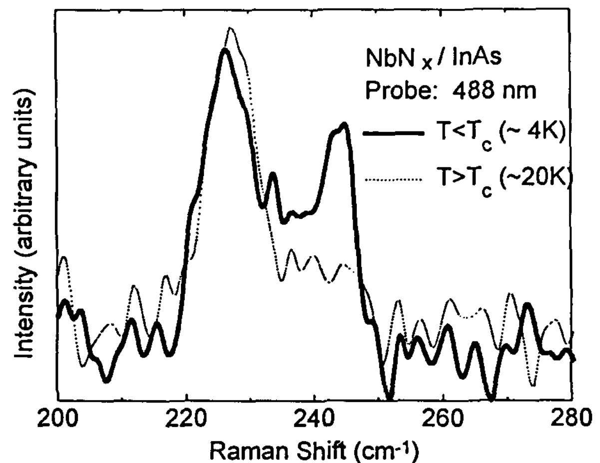

Figure 4. *Temperature-dependent Raman spectra acquired through a NbN_x film reveal a similar enhancement of the LO to L_ phonon mode intensity ratio as seen in Nb/InAs. The T_c of this system is 12K.*

5. DISCUSSION

The Raman data are similar to the results by Ching et. al. [41] who applied a bias voltage across the (100) surface of p-type InAs and saw a change in the LO phonon intensity. They attribute this to the change in the effective scattering volume which coincides with changes in carrier density. In other work, Buchner and Burstein [34] placed n^+-InAs in an electrolytic cell and applied electric fields to either deplete or enhance the accumulated surface. They saw changes in the low frequency coupled mode intensity which were attributed to changes in free carrier concentration, demonstrating that scattering probes the free carrier concentration in the near-surface region. In both of these works, the applied fields significantly changes both the surface and bulk electronic properties. This is different from our work, as we only observe a subtle change in the coupled phonon-plasmon mode relative to the pronounced change in the LO phonon mode.

The observed changes in the Raman spectrum as the superconducting transition is crossed cannot be due to the superconductivity in the Nb metal alone. First, there is no first-order phase transition in the Nb that would place strain on the InAs, since the experiments are all performed in zero applied magnetic field. Second, any changes in the band-structure properties of the Nb are negligible on the energy scale of the Raman scattering experiment: The Nb superconducting gap in our thin films is less than 1 meV, and would have no effect on the visible probing light nor on the ~29 meV Raman shifts. Finally, the changes in the Raman intensity of the LO and L_ modes are only observed when the Nb and InAs are in good electrical contact

We stress that the height and width of the CAR are determined by surface states and doping level. [5] Experiments have verified that the CAR is insensitive to metal deposition, if any. Therefore, the < 1 meV change in the chemical potential, upon the onset of superconductivity, cannot account for the observed effect. We therefore conclude that the observed effect is not merely due to a simple charge transfer between the Nb and InAs upon crossing the superconducting transition.

The increase in LO phonon intensity may be attributed to one or more of the following effects occurring in the surface charge accumulation region: 1) an increase in the scattering volume due to an increase in the width; 2) an increase in the disparity of the electronic properties with the bulk; 3) an increase in the carrier concentration; and 4) a phase correlation of carriers. Each is briefly discussed below.

An increase in the width of the accumulation region would increase the scattering cross-section of the LO phonon with respect to the L- mode. Since the thickness of the accumulated region is supposedly fixed by the level of doping in the InAs, it is difficult to understand how the width of this region changes upon the T_C crossing. The observation of the LO mode itself is due to the disparity of the electronic properties of the near-surface and bulk regions, and it has been suggested that an increase of this disparity would enhance the LO mode. [42] A proximity effect would certainly increase the conductivity of the region of the InAs juxtaposed with the Nb, but it is unclear how this affects the Raman intensity. If charges were transported from the Nb into the InAs, thereby increasing the carrier concentration as listed in 3) above, the Raman cross-section would necessarily be increased in the InAs and the LO mode would be enhanced, but as stated above, there is not obvious mechanism for this. Finally, below the superconducting transition temperature, the electrons and holes in the InAs charge accumulation region must have developed some degree of correlation arising from the Andreev reflection at the interface. Assuming a clean interface and taking into account the differences in the effective masses and Fermi momenta of the two materials, we calculate the ideal probability for Andreev reflection to be 83%. The effect of a correlated electron plasma on the Raman lattice-mode intensity has not been experimentally or theoretically investigated.

6. CONCLUSION

Changes in the electronic character of the near-surface electronic properties of InAs in intimate electrical contact with superconducting Nb are observed by Raman spectroscopy. The LO phonon mode, associated with the charge accumulation layer at the interface, exhibits a marked increase in relative intensity as compared with the L- coupled plasmon-phonon mode, which is primarily associated with the bulk. It is possible that an increase in the carrier concentration in the accumulation layer can account for this effect, but it is also noted that the effect of correlated electrons on Raman cross-section is not known. The observed change in the Raman spectra with temperature must be due to a superconducting proximity effect. We believe this novel optical method of proximity-effect detection is promising for studying the basic physics of superconducting interfaces and for device applications.

ACKNOWLEDGMENTS

The authors are grateful for enlightening discussions on light scattering and transport with G. Blumberg, P. M. Goldbart, A. Kastalsky, M. V. Klein, A. W. Kleinsasser, J. E. Maslar, D. Maslov, A. Pinczuk, J. Sauls, D. J. van Harlingen and D. van der Marel. We thank I. K. Robinson and P. M Miceli for x-ray reflectivity and analysis.

REFERENCES

[1] G. Deutcher and P. G. deGennes in *Superconductivity*, R.D. Parks, ed. (Marcel Dekker, NY, 1969) p1005.

[2] Fei Zhou, B. Spivak and A. Zyuzin, Phys. Rev. B **52**, 4467 (1995).

[3] I. G A. Devyatov and M. Yu. Kupriyanov, JETP Lett. **59**, 200 (1994).

[4] For review, see A. W. Kleinsasser and W. J. Gallagher in *Superconducting Devices*, D. Rudmann and S. Ruggiero, eds., (Academic Press, Boston, 1989) p.325; and T. M. Klapwijk, Physica B **197**, 481 (1994).

[5] For example, see B. G. Streetman, *Solid State Electronic Devices* (Prentice Hall, Englewood Cliffs, NJ, 1990).
[6] J. F. Dorsten, J. E. Maslar, and P. W. Bohn, Appl. Phys. Lett. **66**, 1755 (1995).
[7] L. A. Farrow, C. J. Sandroff, and M. C. Tamargo, Appl. Phys. Lett **51**, 1931 (1987).
[8] J. E. Maslar, J. F. Dorsten, P. W. Bohn, S. Agarwala, I. Adesida, C. Caneau, and R. Bhat, J. Vac. Sci. Tech. B **13**, 988 (1995).
[9] J. Geurts, Surf. Sci. Rep. **18**, 5 (1993).
[10] B. Boudart, B. Prevot, and C. Schwab, Appl. Surf. Sci. **50**, 295 (1991).
[11] P. D. Wang, M. A. Foad, C. M. Sotomayor-Torres, S. Thoms, M. Watt, R. Cheung, C. D. W. Wilkinson, and S. P. Beaumont, J. Appl. Phys. **71**, 3754 (1992).
[12] M. Holtz, R. Zallen, O. Brafman, and S. Matteson, Phys. Rev. B **37**, 4609 (1988).
[13] A. Mlayah, R. Carles, G. Landa, E. Bedel, and A. Munoz-Yague, J. Appl. Phys. **69**, 4064 (1991).
[14] A. Pinczuk, J. M. Worlock, H. L. Stormer, A. C. Gossard, W. Wiegmann, J. Vac. Sci. Tech. **19**, 561 (1981).
[15] J. S. Kim, D. G. Seiler, and W. F. Tseng, J. Appl. Phys. **73**, 8324 (1993).
[16] J. F. Dorsten, T. A. Tanzer, P. W. Bohn, A. C. Abeyta, I.V. Roshchin, and L. H. Greene, preprint.
[17] L. H. Greene, A. Abeyta, I. V. Roshchin, I. K. Robinson, J. F. Dorsten, T. A. Tanzer and P. W. Bohn in "*Spectroscopic Studies of Superconductors*", Ivan Bozovic and Dirk van der Marel, eds. SPIE Vol. **2696**, (SPIE, Bellingham, WA, 1996) p215.
[18] L. H. Greene, J. F. Dorsten, I. V. Roshchin, A. C. Abeyta, T. A. Tanzer, W. L. Feldmann and P. W. Bohn, Czechoslovak Journal of Physics **46**, Suppl. S2, 741 (1996).
[19] A. F. Andreev, Sov. Phys JETP **19**, 1228 (1964). [J. Exptl. Theoret. Phys. (U.S.S.R.)].
[20] A. Kastalsky, A. W. Kleinsasser, L. H. Greene, R. Bhat, F. P. Milliken, and J. B. Harbison, Phys. Rev. Lett. **67**, 3026 (1991).
[21] G. E. Blonder, M. Tinkham, and T. M. Klapwijk, Phys. Rev. B **25**, 4515 (1982).
[22] T. M. Klapwijk, G. E. Blonder, M. Tinkham, Physica B+C **109-110**, 1657 (1982).
[23] A. W. Kleinsasser, T. N. Jackson, D. McInturff, F. Rammo, G. D. Pettit and J. M. Woodall, Appl. Phys. Lett. **57**, 1811 (1990).
[24] F. E. Aspen and A. M. Goldman, J. Low Temp. Phys. **43**, 559 (1981).
[25] M. Kadin and A. M. Goldman, Phys. Rev. B **25**, 6701 (1982).
[26] B. J. van Wees, P. de Vries, P. Magnée, and T. M. Klapwijk, Phys. Rev. Lett. **69**, 510 (1992).
[27] I. K. Marmorkos, C. W. J. Beenakker, and R. A. Jalabert, Phys. Rev. B **48** 2811 (1993).
[28] H. Takayanagi and T. Kawakami, Phys. Rev. Lett. **54**, 2449 (1985).
[29] K. Inoue and H. Takayanagi, Phys Rev. B. **43**, 6214 (1991).
[30] J. Nitta, T. Akazaki, H. Takayanagi, and K. Arai, Phys. Rev. B **46**, 14,286 (1992).
[31] H. Takayanagi, J. B. Hansen and J. Nitta, Phys. Rev. Lett. **74**, 162 (1995).
[32] C. Nguyen, J. Werking, H. Kroemer, and E. L. Hu, Appl. Phys. Lett. **57**, 87 (1990).
[33] C. Nguyen, H. Kroemer, and E. L. Hu, Phys. Rev. Lett. **69**, 2847 (1992).
[34] S. Buchner and E. Burstein, Phys. Rev. Lett. **33**, 908 (1974).
[35] M. Noguchi, K. Hirakawa, and T. Ikoma, Phys. Rev. Lett. **66**, 2243 (1991).
[36] C. K. N. Patel and R. E. Slusher, Phys Rev, Lett. **167**, 413 (1968).
[37] Y. B. Li, I. T. Ferguson, R. A. Stradling, and R. Zaalen, Semicond. Science. and Technol. **7**, 1149 (1992).
[38] D. Olego and M. Cardona, Phys. Rev. B **24**, 7217 (1981).
[39] H. Shen, F. Pollak, and R. N. Sacks, SPIE Proc. **524**, 145 (1985).
[40] P. Corden, A. Pinczuk, and E. Burstein, Proc. 10th Intl. Conf. Phys. Semicond., S.P. Keller, J.C. Hensel, F. Stern, eds., 739 (1970).
[41] L. Y. Ching, E. Burstein, S. Buchner, and H. H. Wieder, J. Phys. Soc. Jpn **49**, 951 (1980).
[42] A. Pinczuk, private communications.